

Cardiac magnetic resonance longitudinal strain analysis in acute ST-segment elevation myocardial infarction: A comparison with speckle-tracking echocardiography

Filipa Valente^{a,*}, Laura Gutierrez^a, Lucia Rodríguez-Eyras^a, Rúben Fernandez^a, Maria Montano^a, Augusto Sao-Aviles^a, Victor Pineda^b, Andrea Guala^a, Hug Cuéllar^b, Arturo Evangelista^a, José Rodríguez-Palomares^a

^a Cardiology Department, Hospital Universitari Vall d'Hebron, Barcelona, Spain¹

^b Radiology Department, Hospital Universitari Vall d'Hebron, Barcelona, Spain¹

ARTICLE INFO

Article history:

Received 23 February 2020

Accepted 1 June 2020

Keywords:

Myocardial deformation
Longitudinal strain
Feature-tracking
Cardiac magnetic resonance
Speckle-tracking echocardiography

ABSTRACT

Background: Strain analysis with speckle-tracking echocardiography (STE) is considered superior to ejection fraction for ventricular function assessment in different clinical scenarios. Feature tracking (FT) permits cardiac magnetic resonance (CMR) strain analysis in routinely acquired cine images. This study evaluated the feasibility of CMR-FT and its agreement with STE in patients with acute ST-segment elevation myocardial infarction (STEMI).

Methods: An echocardiogram and CMR were performed in 128 patients who underwent primary percutaneous revascularisation after a STEMI. Adequate strain analysis was obtained by both techniques in 98 patients and peak systolic longitudinal strain (LS) was assessed with STE and CMR-FT.

Results: Of 1568 myocardial segments, 97.2% were correctly tracked with STE and 97.7% with CMR-FT. For global LS, STE showed a mean of $-14.8 \pm 3.3\%$ and CMR-FT $-13.7 \pm 3.0\%$, with good agreement between modalities [intraclass correlation coefficient (ICC) 0.826; bias -1.09% ; limits of agreement (LOA) $\pm 4.2\%$]. On the other hand, segmental LS agreement was only moderate, with an ICC of 0.678 (bias -1.14% ; LOA $\pm 11.76\%$) and the ICC ranged from 0.538 at the basal antero-lateral segment to 0.815 at the apical lateral segment. Finally, both STE and CMR-FT showed excellent intra- and inter-observer reproducibility (ICC > 0.9).

Conclusions: CMR-FT provides LS with similar feasibility to STE and both techniques showed good agreement for global LS, although agreement at segmental level was only moderate. CMR-FT showed excellent reproducibility, strengthening its robustness and potential for both research and clinical applications.

© 2020 The Authors. Published by Elsevier B.V. This is an open access article under the CC BY-NC-ND license (<http://creativecommons.org/licenses/by-nc-nd/4.0/>).

1. Introduction

Left ventricular (LV) myocardial strain imaging refers to the quantification of myocardial deformation, i.e. to the fractional shortening/lengthening and thickening/thinning of the myocardial wall throughout the cardiac cycle. It is a measurement of global and segmental LV function and has been shown to be an earlier marker of myocardial dysfunction than wall motion abnormalities or ejection fraction (EF).

The main body of evidence has been mostly gathered for longitudinal strain (LS) derived from speckle-tracking echocardiography (STE), which is widely used and provides diagnostic and prognostic information in several diseases such as in cardiomyopathies [1–3], valvular heart disease [4], cardiotoxicity [5] and congenital heart diseases [6]. In acute ischaemic heart disease, STE is a good predictor of left ventricular remodelling and adverse cardiovascular events [7,8].

Cardiac magnetic resonance (CMR) is also widely used in ischaemic heart disease for the assessment of global and segmental LV function, infarct transmural and microvascular obstruction. Deformation analysis has been used for several decades, although initial techniques such as myocardial tagging did not find widespread application due mainly to the need for further pulse acquisitions and time-consuming analysis [9]. More recently, feature

* Corresponding author at: Hospital Universitari Vall d'Hebron, Passeig Vall d'Hebron, 119-129, 08035 Barcelona, Spain.

E-mail address: filipaxavievalente@gmail.com (F. Valente).

¹ This author takes responsibility for all aspects of the reliability and freedom from bias of the data presented and their discussed interpretation.

tracking has been applied to routine CMR cine sequences, with no further sequence acquisition needed, offering a higher signal-to-noise ratio and unlimited acquisition window compared to STE. Although these advantages may enable a wider use of CMR strain, the relationship between STE and CMR strain remains to be clearly established.

The aim of this study was to evaluate the feasibility and reproducibility of LS analysis with CMR feature tracking (CMR-FT) and to compare it with STE in patients with acute ST-segment elevation myocardial infarction (STEMI).

2. Methods

The present study included patients from a single tertiary centre enrolled in a large double-blind randomized clinical trial in which after admission with a STEMI they were randomized to receive 4.5 mg of adenosine or saline intracoronary injection immediately prior to PCI [10]. Acute STEMI was defined according to published guidelines [11]. All patients underwent coronary angiography within 6 h of chest pain onset and primary percutaneous coronary intervention was performed in all patients following international guideline recommendations. Patients were included if they presented an initial TIMI 0 or I anterograde flow in the culprit artery and a final TIMI III flow. Complete revascularization was achieved in all patients. Major exclusion criteria were previous myocardial infarction, renal function <30 mL/min/1.73 m² and permanent atrial fibrillation. Within 3–5 days of the myocardial infarction, patients underwent echocardiography and CMR, with an interval of <24 h between studies. All procedures complied with the Declaration of Helsinki and were approved by our local Ethics Committee. All patients gave their written informed consent.

2.1. Echocardiography examination

Echocardiography was performed using a commercially-available standard ultrasound scanner (Vivid 9, GE Vingmed Ultrasound AS) with a 3.5 MHz transducer. A standard protocol was used according to international societies' recommendations

[12,13]. Using the AHA 16-segment model, a wall motion score (WMS) was attributed to each segment (normokinesis 1, hypokinesis 2, akinesis 3), and an average wall motion score index (WMSI) was calculated.

2.2. Speckle-tracking analysis

For STE analysis, dedicated 2D image loops were acquired of three stable consecutive cardiac cycles during breath-hold in apical 2-, 3- and 4-chamber views, with a frame rate of 60–80 frames/s. A pulse-wave Doppler recording through the LV outflow tract was acquired from a 5-chamber view to identify the systolic interval, defined as the time between aortic valve opening and closure [14]. All recordings were stored digitally and analysed off-line using standard software (EchoPAC PC, version 11.0, GE Healthcare). A region of interest was defined in each view by tracing the endocardium, and the software then automatically tracked each segment. Manual adjustments were made if deemed necessary; however, if tracking quality remained inadequate, the segment was excluded from the analysis. The automatic algorithm generated strain curves for each of the 16 segments, from which segmental and global LS values were obtained (Fig. 1). As LS refers to apex-to-base shortening, the reduction in myocardial fibre length is represented by negative values; nevertheless, unless stated otherwise, we will refer to absolute measurement values. One experienced echocardiographer (LG) performed all STE analyses.

2.3. CMR examination

CMR was performed in a clinical 1.5 T whole-body MR scanner (Magnetom Symphony, Siemens) using a dedicated cardiac phased-array receiver coil. The standardized study protocol included 2D balanced steady-state free precession (b-SSFP) cine images in 2-, 3- and 4-chamber long-axis planes and a stack of short-axis images from the mitral valve to the apex (TR 3.2 ms, TE 1.5 ms, spatial resolution $1.4 \times 1.4 \times 8.0$ mm, retrospective ECG gating, temporal resolution 28–37 msec, 25 phases per cardiac cycle and 7–12 s of breath-hold time per image). Late gadolinium-enhancement (LGE) was analysed for infarct size quantification

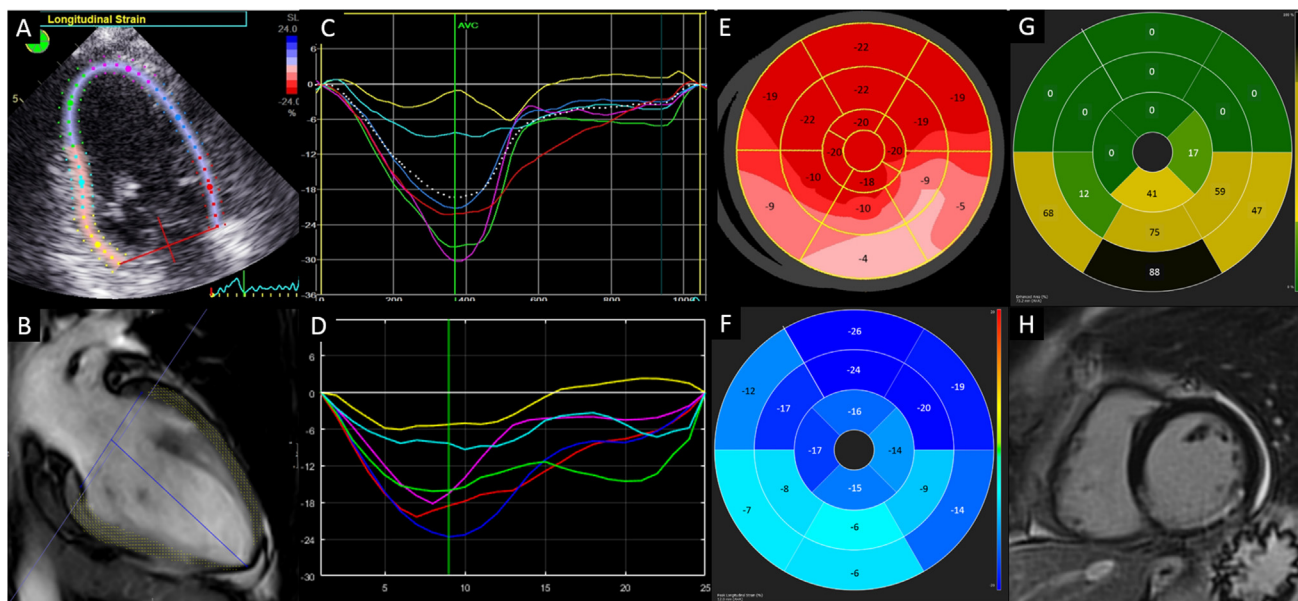


Fig. 1. Inferior STEMI. A and B, end-diastolic 2-chamber strain analysis with STE and CMR-FT, respectively. C and D, 2-chamber STE and CMR-FT strain curves showing lower values for infarcted segments (yellow and light blue curves). E and F, bull's eye plots representing LS from STE and CMR-FT, respectively. G, bull's eye plot of the extent of late gadolinium enhancement (LGE, %). H, LGE image at a basal short-axis level showing the inferior STEMI.

with 2D segmented inversion-recovery gradient echo sequences in the same imaging planes, acquired 20 min after intravenous administration of 0.2 mmol/kg of gadobutrol (spatial resolution $1.4 \times 1.4 \times 8.0$ mm, end-diastolic phase). Quantification was performed using the 5-SD technique [15] with manual correction as deemed necessary and inclusion of no-reflow zones. All data were stored in DICOM format and analysis was made off-line.

2.4. Feature tracking analysis

Myocardial deformation analysis was made with Tissue Tracking (CVI42[®], version 5.2.1, Circle Cardiovascular Imaging) using standard b-SSFP cine images. The endocardial and epicardial borders were manually traced in the end-diastolic phase of the three long-axis and the short-axis stack. The most basal slice of the short-axis stack to be included was the first that did not present any distortion from the LV outflow tract throughout the cardiac cycle. The anterior insertion of the right ventricle in the short axis-slices was used to define the segments according to the AHA 16-segment model. The software automatically tracks tissue features throughout all phases and generates myocardial deformation curves (Fig. 1). If wall motion tracking was considered inadequate, minor adjustments were made. If these failed, the segment was excluded from the final analysis. As for STE, the systolic interval was identified by aortic valve opening and closure as observed in 3-chamber cine images [14]. One cardiologist dedicated to CMR (FV) performed all CMR-FT analyses.

2.5. Reproducibility

Thirty patients were randomly selected to determine intra- and inter-observer variability of CMR-FT and STE strain analysis. Two experienced investigators independently analysed the same echocardiography and CMR images (LG and RF for STE, and FV and LR for CMR-FT) and one investigator of each pair (RF and FV, respectively) repeated the analysis one month later to assess intra-observer agreement.

2.6. Statistical analysis

Continuous variables are presented as mean \pm standard deviation (SD). Comparison between STE and CMR-FT strain was made using a paired Student's *t*-test. Agreement between the two imaging modalities was determined by calculating mean bias and 95% limits of agreement (LOA) from Bland-Altman statistics [16], and intraclass correlation coefficient (ICC). Correlation of strain values with other CMR parameters was performed with Pearson's correlation test. Intra- and inter-observer reproducibility was assessed using ICC and Bland-Altman statistics. Reliability was considered poor if the ICC was <0.5 , moderate from 0.50 to 0.75, good from 0.75 to 0.9 and excellent if >0.90 [17]. A *p*-value <0.05 was considered statistically significant. All statistical analyses were performed with SPSS 19.0 (SPSS Inc, Chicago, Illinois).

3. Results

One hundred and thirty-five patients were included in the study. All underwent echocardiography; however, 7 (5%) could not undergo CMR owing to severe claustrophobia. Nineteen (14%) remaining patients were excluded due to sub-optimal acoustic window, deemed insufficient for STE analysis, and 11 (8%) because of images inadequate for CMR-FT analysis due to severe cardiac and/or respiratory motion artefacts. Mean interval between echocardiography and CMR was 6.2 ± 2 h and no complications

Table 1

Baseline clinical characteristics, angiographic findings and conventional CMR parameters (*n* = 98).

Clinical characteristics	
Age, years	58 \pm 13
Male sex, <i>n</i> (%)	88 (90%)
Hypertension, <i>n</i> (%)	57 (58%)
Diabetes mellitus, <i>n</i> (%)	20 (20%)
Dyslipidaemia, <i>n</i> (%)	33 (34%)
Smoking, <i>n</i> (%)	53 (54%)
Body mass index, kg/m ²	28.2 \pm 6.7
Angiographic findings	
Culprit artery, <i>n</i> (%)	
RCA	42 (43%)
LAD	43 (44%)
LCx	13 (13%)
Time to reperfusion, min	211 \pm 68
CMR parameters	
LVEDV (mL)	157.4 \pm 33.6
LVESV (mL)	78.9 \pm 27.2
LVEF (%)	50.6 \pm 9.7
WMSI	1.6 \pm 0.3
LV mass (g)	128.1 \pm 25.9
LV infarct mass (g)	28.4 \pm 23.6
Relative infarct mass (%)	21.6 \pm 4.1

LAD, left anterior descending artery. LCx, left circumflex artery. LV, left ventricle. LVEDV, left ventricular end-diastolic volume. LVEF, left ventricular ejection fraction. LVESV, left ventricular end-systolic volume. RCA, right coronary artery. WMSI, wall motion score index.

related to either procedure occurred. Baseline characteristics of the final 98 patients are shown in Table 1.

3.1. Feasibility of STE and CMR-FT myocardial segment analysis

Of 1568 myocardial segments, 1524 (97.2%) were correctly tracked with STE and 1532 with CMR-FT (97.7%). Poor tracking with STE occurred mainly at the basal segments where 19 were excluded (43% of 44 excluded segments). For CMR-FT, the 36 excluded segments were mostly basal anterior (*n* = 10), antero-septal (*n* = 20) and infero-septal (*n* = 3). Off-line analysis time with STE was 197 ± 33 s (range: 142–245 s) and with CMR-FT 287 ± 31 s (range: 235–353 s).

3.2. Global peak systolic longitudinal strain

STE analysis of peak systolic global longitudinal strain (GLS) showed a mean of $-14.8 \pm 3.3\%$ with a range from -22% to -5% . CMR-FT GLS was slightly lower with a mean of $-13.7 \pm 3.0\%$ (*p* = 0.016), with a range from -21% to -5% . Agreement between imaging modalities was good, with an ICC of 0.826 (95% confidence interval of 0.682–0.899, *p* < 0.001). Bland-Altman analysis showed a small bias of -1.09% with $\pm 4.2\%$ of limits of agreement (Fig. 2).

Agreement between both techniques was good irrespective of presence of left ventricular systolic dysfunction (ICC 0.828 for LVEF $< 57\%$ and ICC of 0.744 for LVEF $\geq 57\%$; Fig. 3A) or left ventricular dilatation (ICC 0.836 for non-dilated and ICC of 0.849 for dilated left ventricle; Fig. 3B).

GLS according to the STEMI culprit vessel was significantly lower with both STE and CMR-FT in patients with LAD-STEMI compared to RCA-STEMI (Table 2). Agreement between techniques was good, particularly for LAD-STEMI (ICC 0.876).

Correlation of GLS with other CMR parameters, namely WMSI, LVEF and relative infarct mass was moderate for both techniques (Fig. 4).

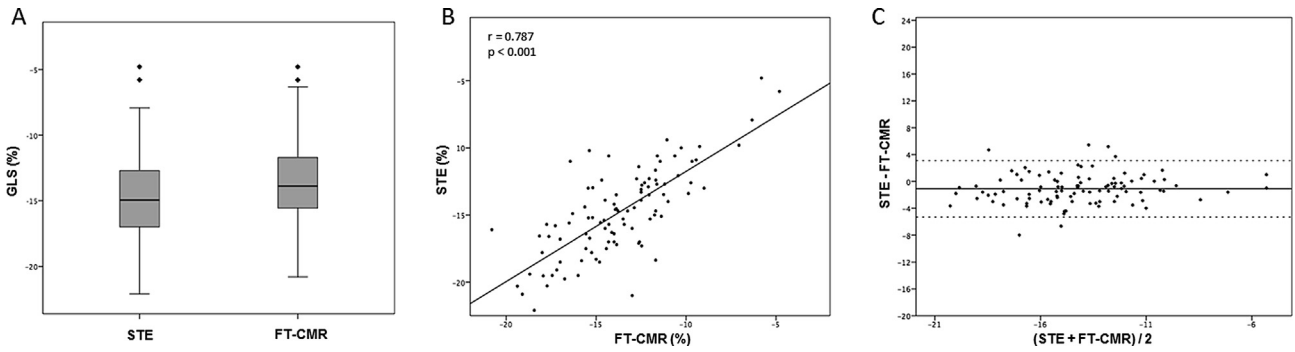


Fig. 2. Comparison of global LS measured with STE and CMR-FT. (A) Boxplot analysis. (B) Linear correlation. (C) Bland-Altman analysis.

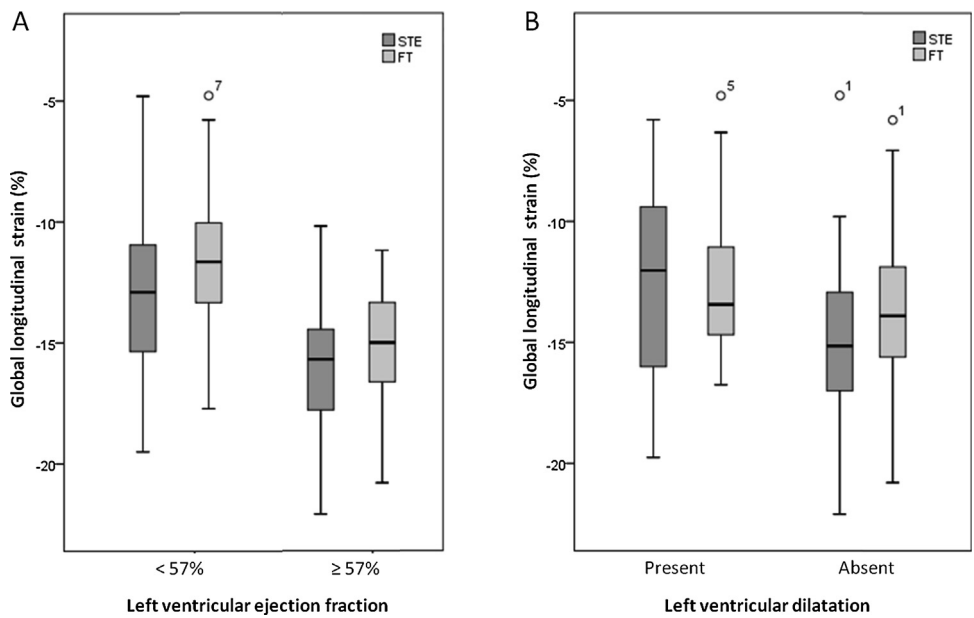


Fig. 3. Comparison of global LS measured with STE and CMR-FT according to (A) presence of left ventricular systolic dysfunction (LVEF < or ≥ 57%) and (B) presence of left ventricular dilatation, defined as end-diastolic volume > 97 mL/m² in women and > 106 mL/m² in men.

Table 2
Global LS according to STEMI culprit vessel.

	STE	CMR-FT	p	ICC	p
LAD	-13.12 ± 3.2	-12.51 ± 3.3	0.000	0.876 (0.769–0.933)	0.000
RCA	-16.45 ± 2.6*	-14.93 ± 2.3*	0.000	0.658 (0.231–0.834)	0.000
LCx	-14.81 ± 2.9	-13.52 ± 2.4	0.000	0.696 (0.093–0.904)	0.015

LAD, left anterior descending artery; LCx, left circumflex artery. LS, longitudinal strain; RCA, right coronary artery.
*p < 0.05 compared with LAD.

3.3. Segmental peak systolic longitudinal strain

STE analysis of 1524 segments showed a mean peak segmental LS of -14.7 ± 6.3%, with a minimum of -37.5% and a maximum of 4.5%. CMR-FT LS was lower with a mean of -13.6 ± 5.9% (p < 0.01), a minimum of -38% and a maximum of 5.0%. Agreement between modalities was moderate with an ICC of 0.678 (0.637–0.714, p < 0.001), and Bland-Altman analysis showed a mean difference of -1.14% with LOA of ±11.76% (Fig. 5).

Segmental LS analysis is shown in Table 3. Significant agreement was found between modalities for all segments; however, the level of agreement varied greatly according to the myocardial segment,

with an ICC ranging from 0.538 at the basal antero-lateral segment to 0.815 at the apical lateral segment. Overall, 3 segments showed good agreement (ICC > 0.75) while agreement was moderate for the remaining segments (ICC from 0.538 to 0.724).

Analysis according to ventricular level (basal, mid and apical) is shown in Fig. 6. Significant agreement was observed for all levels and ICC correlation was the lowest for basal segments and the highest for apical segments.

For all segments, analysis of myocardial deformation according to wall motion score categories revealed progressive worsening of LS with worsening myocardial contractility (Table 4). Similarly, LS decreases with increasing infarct transmuralty (Table 5).

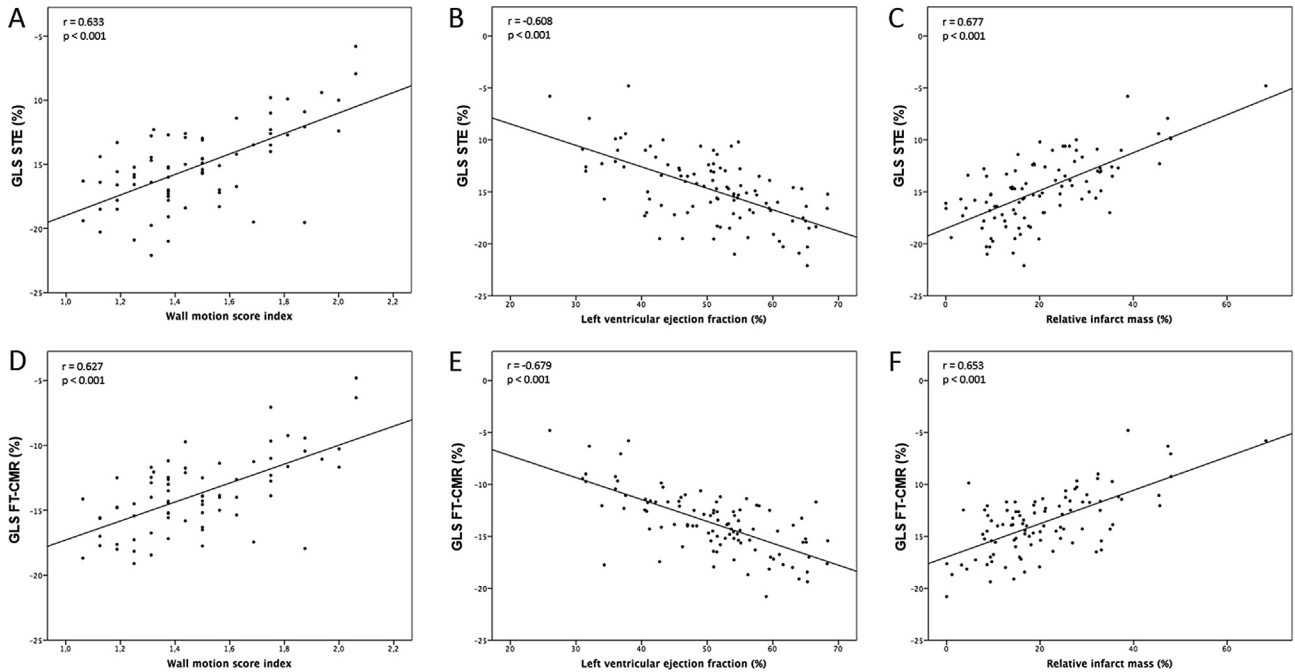


Fig. 4. Linear correlation analysis comparing STE and CMR-FT GLS with WMSI (A and D, respectively), LVEF (B and E, respectively) and relative infarct mass (C and F, respectively).

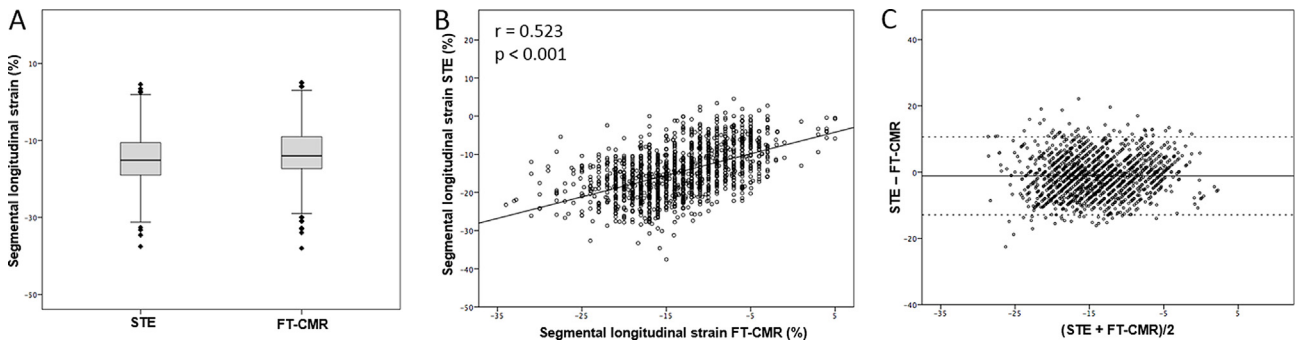


Fig. 5. Comparison of segmental LS measured with STE and CMR-FT. (A) Boxplot analysis. (B) Linear correlation. (C) Bland-Altman analysis.

3.4. Intra- and inter-observer variability of STE and CMR-FT

Results for intra- and inter-observer variability are shown in Table 6. STE and CMR-FT showed excellent reproducibility at both global and segmental level.

4. Discussion

The current study demonstrated that (a) CMR-FT global and segmental LV strain can be quantified with similar feasibility as STE; (b) in patients with STEMI, CMR-FT and STE had good agreement in global LS quantification, while only moderate in segmental analysis; and (c) both techniques showed excellent reproducibility.

4.1. Myocardial strain analysis and feasibility

Myocardial strain analysis is a post-processing technique that translates deformation of the myocardium during the cardiac cycle into a percentage of its initial length. Although strain can be derived from both echocardiography and CMR, the physical principles underlying each technique are quite different.

STE is based on tracking of natural acoustic markers known as “speckles” which originate from the backscatter of ultrasound within myocardial tissue and are relatively stable throughout the cardiac cycle [18,19]. Nevertheless, STE is limited by spatial resolution, it is highly dependent on image quality and temporal resolution, and the signal dropout of distal segments may be a concern.

For CMR, an approach to strain analysis based on tracking of MRI patterns or features such as the endocardial-blood pool border has recently been developed [18,19]. These so-called “feature-tracking” algorithms are available from different vendors and can be applied to cine sequences routinely acquired for ventricular volumes and EF calculation. Therefore, these algorithms do not lengthen the CMR study and permit retrospective analysis of past studies. Compared to echocardiography, CMR benefits from a better signal-to-noise ratio, is unrestrained by “window” quality and relies on integration of information from long-axis and short-axis images.

In the present study, the feasibility of LS assessment was similar with CMR-FT and STE (97.7% vs 97.2%, respectively). These results are in line with those of previous studies with STE that showed 89–100% correct tracking [20–23] and 90–100% in studies with CMR feature-tracking [21–26]. Regional analysis of STE revealed the worst tracking feasibility for basal segments possibly as a

Table 3
Segmental LS and intra-class correlation coefficient (ICC) between STE and CMR-FT.

Segments	STE (%)	CMR-FT (%)	p-value	ICC	p-value
1. Basal anterior	-14.87 ± 5.6	-12.89 ± 5.5	0.000	0.717 (0.537–0.825)	<0.001
2. Basal antero-septal	-13.98 ± 5.9	-12.20 ± 4.2	0.000	0.574 (0.333–0.729)	<0.001
3. Basal infero-septal	-12.71 ± 4.4	-13.90 ± 5.0	0.000	0.564 (0.350–0.709)	<0.001
4. Basal inferior	-14.70 ± 6.4	-16.26 ± 7.4	0.000	0.654 (0.484–0.768)	<0.001
5. Basal infero-lateral	-15.95 ± 6.4	-17.72 ± 5.4	0.000	0.561 (0.344–0.706)	<0.001
6. Basal antero-lateral	-16.06 ± 5.5	-15.12 ± 5.3	0.000	0.538 (0.307–0.693)	<0.001
7. Mid anterior	-14.15 ± 6.5	-13.88 ± 5.8	0.000	0.786 (0.676–0.859)	<0.001
8. Mid antero-septal	-15.16 ± 6.7	-13.18 ± 4.6	0.000	0.724 (0.563–0.822)	<0.001
9. Mid infero-septal	-14.58 ± 4.6	-11.97 ± 4.5	0.000	0.559 (0.266–0.726)	<0.001
10. Mid inferior	-14.45 ± 5.9	-12.84 ± 5.6	0.000	0.665 (0.497–0.777)	<0.001
11. Mid infero-lateral	-14.17 ± 5.6	-14.73 ± 5.8	0.000	0.611 (0.417–0.740)	<0.001
12. Mid antero-lateral	-14.26 ± 5.6	-14.96 ± 5.5	0.000	0.629 (0.440–0.754)	<0.001
13. Apical anterior	-15.06 ± 8.6	-12.51 ± 6.6	0.000	0.809 (0.659–0.886)	<0.001
14. Apical septal	-15.80 ± 6.9	-11.36 ± 5.2	0.000	0.699 (0.135–0.863)	<0.001
15. Apical inferior	-16.48 ± 7.4	-11.08 ± 5.7	0.000	0.599 (0.010–0.807)	<0.001
16. Apical lateral	-13.07 ± 7.2	-12.45 ± 7.1	0.000	0.815 (0.723–0.876)	<0.001

consequence of signal dropout. CMR-FT also showed worse basal segment tracking, and contributing factors may have included interference of LV outflow tract deformation and the complex mitral annular anatomy associated with very rapid movement of adjacent basal segments [18,27].

4.2. Global longitudinal strain analysis

Comparison of GLS quantification with STE and CMR-FT has been reported, with different results depending on the clinical setting and sample size. Obokata et al. [23] compared CMR feature tracking with STE in an all-comer population and observed a high correlation for GLS ($r=0.83$), but only a small proportion of patients had ischaemic heart disease. On the other hand, Orwat et al. [28] found only a moderate correlation (ICC 0.57, CoV 14.4%) in a small population with hypertrophic cardiomyopathy and, strikingly, Lamacie et al. [21] reported poor results in thalassaemia major patients ($r=0.25$, $p=0.16$).

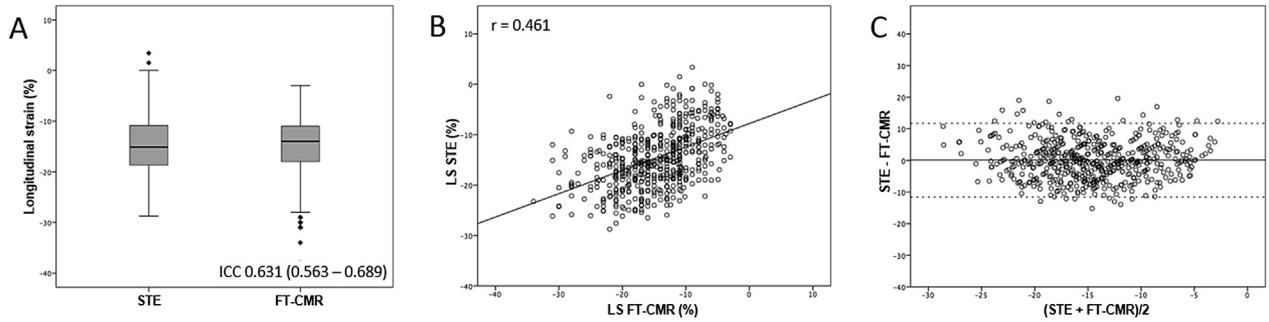
To the best of our knowledge, this is the first study to compare global and segmental LS between STE and CMR in a large population of acute ischaemic heart disease patients. We found that CMR-FT yielded slightly lower values than STE ($-14.8 \pm 3.3\%$ vs $13.7 \pm 3.0\%$, $p=0.016$). Amongst other factors, this could be a result of the lower temporal resolution of CMR-FT, since short-lived phases such as peak systole or peak isovolumetric contraction/relaxation could be missed. However, the impact of temporal resolution is probably attenuated by the noise-reduction algorithms employed in STE amongst other differences between both techniques and our results do not differ significantly from studies using a higher CMR temporal resolution [27]. Overall, our comparison of GLS showed good agreement between modalities (ICC 0.826, $r=0.787$). This is a significant first step towards the clinical implementation of CMR-FT since, if strain values from both techniques are comparable, CMR-FT may constitute a useful alternative in

patients unsuitable for STE analysis. Additionally, if intermodality agreement is good, the prognostic value of STE would also be expected to be evident for CMR-FT; further studies are required to confirm this hypothesis [29].

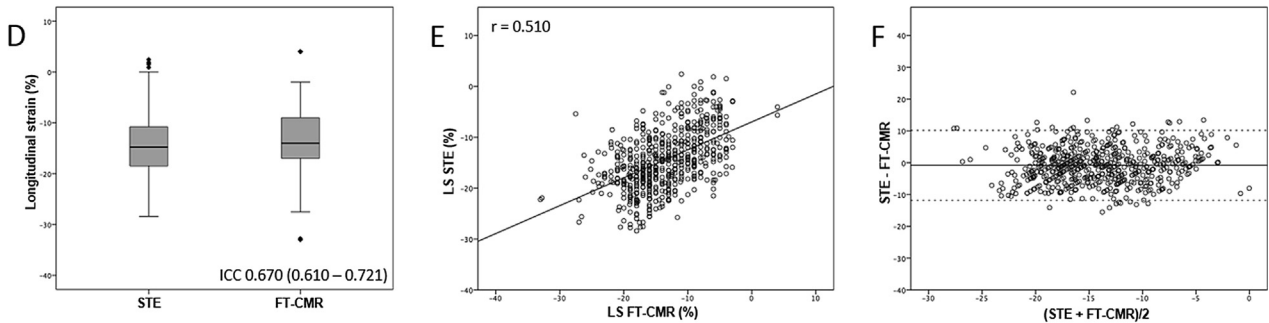
4.3. Segmental longitudinal strain analysis

Segmental LS strain can provide important information in clinical contexts such as ischaemic cardiomyopathy, LV hypertrophy and intraventricular dyssynchrony. Nevertheless, intermodality comparative data are scant and mostly disappointing [27,30]. In this study, all 16 AHA myocardial segments were compared, and moderate agreement found between techniques (ICC = 0.678), varying from 0.538 to 0.815 according to the segment. Although suboptimal, these results are in the range of those observed with intervender STE comparisons. Mirea et al. [20] compared measurements obtained with 6 different ultrasound machines and 8 post-processing softwares and found significant intervender bias (up to -4.6% of absolute difference) and limits of agreement (up to $\pm 7.5\%$), and the ICC ranged from poor to good (0.52–0.79). Several factors may contribute to this variability: differences in the algorithm definition of LS (endocardial-only, mid-wall or whole myocardium), noise reduction and smoothing algorithms [20] and in the imaging planes used for analysis (one long-axis or three long-axes for STE vs. integrated information from 3 long-axes plus the short-axis stack for CMR-FT). Although these factors also affect GLS, the averaged result over a larger myocardium region attenuates range differences and improves intermodality agreement. Segmentation misalignment, which would not affect GLS, can also be a source of error for segmental strain comparison. Finally, basal segments showed the worst agreement, probably a result of the fact that both techniques suffer from poorer tracking in this region. These results call for caution when interpreting and comparing isolated segmental strain values; in the absence of a widespread

Basal level



Midventricular level



Apical level

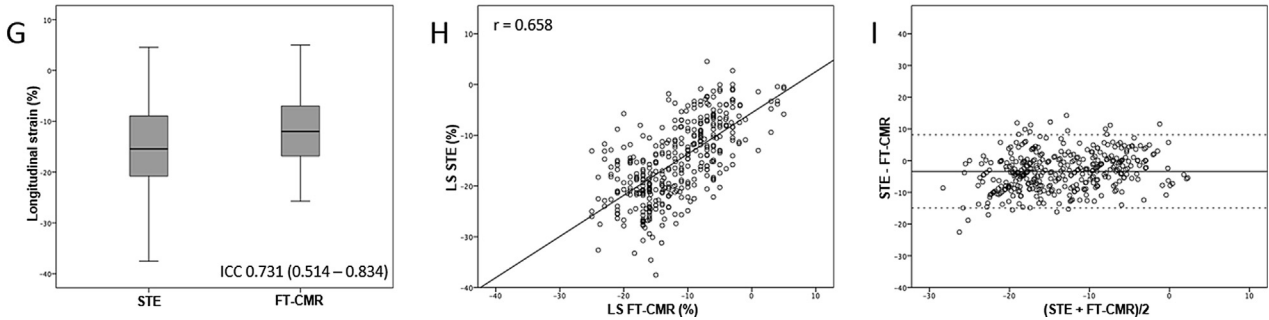


Fig. 6. Comparison of LS measured with STE and CMR-FT per ventricular level. A, D and G, Boxplot analysis. B, E and H, Linear correlation. C, F and I, Bland-Altman analysis.

Table 4

Segmental LS and intraclass correlation coefficient (ICC) between STE and CMR-FT according to wall motion score.

Wall motion score	STE	CMR-FT	ICC	p-value
Normokinesis	-16.86 ± 5.5	-15.48 ± 5.2	0.510 (0.436–0.573)	0.000
Hypokinesis	-13.60 ± 4.6*	-11.41 ± 5.2*	0.348 (0.072–0.545)	0.007
Akinesis	-8.93 ± 5.2*†	-8.90 ± 5.3*†	0.582 (0.487–0.660)	0.000

* p < 0.05 compared with normokinesis; † p < 0.05 compared with hypokinesis.

Table 5

Segmental LS and intra-class coefficient (ICC) correlation between STE and CMR-FT according to infarct transmuralty.

Infarct transmuralty	STE (%)	CMR-FT (%)	ICC	p-value
0–25%	-17.02 ± 5.4	-15.31 ± 5.3	0.508 (0.421–0.580)	<0.001
26–50%	-11.86 ± 5.2*	-11.01 ± 4.9*	0.534 (0.375–0.653)	<0.001
51–75%	-8.48 ± 5.2*†	-9.25 ± 5.2*†	0.509 (0.335–0.637)	<0.001
76–100%	-7.49 ± 4.5*†	-7.34 ± 4.9*†‡	0.584 (0.391–0.715)	<0.001

* p < 0.05 compared to 0–25% infarct transmuralty; † p < 0.05 compared to 26–50% infarct transmuralty; ‡ p < 0.05 compared to 51–75% infarct transmuralty.

Table 6
Intra- and inter-observer variability of GLS measured with STE and CMR-FT.

Global LS	STE			CMR-FT		
	ICC	p-value	Bias ± LOA	ICC	p-value	Bias ± LOA
Intra-observer variability	0.997 (0.993–0.998)	0.000	−0.153 ± 1.06	0.995 (0.989–0.997)	<0.001	0.016 ± 1.09
Inter-observer variability	0.969 (0.935–0.985)	0.000	0.091 ± 3.39	0.990 (0.979–0.995)	<0.001	0.048 ± 1.47
Segmental LS	ICC	p-value	Bias ± LOA	ICC	p-value	Bias ± LOA
Intra-observer variability	0.976 (0.972–0.980)	0.000	−0.157 ± 4.39	0.977 (0.972–0.981)	<0.001	−0.016 ± 4.04
Inter-observer variability	0.920 (0.904–0.933)	0.000	0.154 ± 7.85	0.941 (0.929–0.950)	<0.001	−0.049 ± 6.24

ICC, intraclass correlation coefficient. LOA, limits of agreement. LS, longitudinal strain.

reference standard, further studies assessing the prognostic value of each modality will determine the value of each modality’s segmental strain.

Finally, in this study segmental LS was found to correlate with increasing infarct transmural. We believe the value of segmental LS to predict functional recovery and viability to be an area of great potential for CMR-FT; however, this analysis was beyond the scope of the current study.

4.4. Reproducibility

Previous studies showed high reproducibility of CMR GLS (ICC ≥ 0.85 [21]). In our study, both STE and CMR-FT showed excellent intra- and inter-observer reproducibility for GLS. Regarding segmental strain, previous studies showed conflicting and mostly suboptimal reproducibility for both STE [20,31] and CMR-FT [24,25,30]. Nevertheless, we found excellent intra- and interobserver reproducibility for both. These results may be related to improvements in the contemporary versions of the software as well as the integration of long-axis and short-axis information.

4.5. Clinical implications

Strain analysis with STE, despite some limitations, has been widely implemented in clinical practice and has an established role in the management of different diseases [5,32–35]. Our study demonstrated that CMR-FT GLS showed good agreement with STE in a large population with acute ischaemic heart disease. The most obvious patients to benefit from CMR-FT are those with a poor acoustic window. Nevertheless, the advantages of CMR over echocardiography are largely known; its better signal-to-noise ratio, image quality and low operator dependence render it the goldstandard for EF and LV volume assessment. We expect these advantages to also apply to strain analysis and therefore translate into superior diagnostic and prognostic value; however, further studies are required to confirm this hypothesis. Additionally, ischaemic heart disease patients in whom contrast administration and LGE infarct size quantification are precluded owing to advanced kidney disease may also benefit from CMR-FT for the estimation of infarct transmural, although the correlation and predictive value of strain in this context needs to be confirmed. Ultimately, the agreement between both modalities means that individual patients can be monitored alternately with either, and extension to other diseases could result in the definition of disease-related cut-offs to guide patient management.

4.6. Limitations

Although myocardial tagging is considered the reference standard for deformation analysis, we compared CMR-FT with STE

because we considered the latter to be a more clinically significant and pragmatic reference standard, since it is the only technique widely implemented in clinical practice. For the same reason, our study was focused exclusively on LS, although circumferential and radial strains are also easily obtained with CMR-FT [36]. Finally, although both techniques showed excellent reproducibility, true test-retest variability was not assessed since this was a retrospective study. However, we believe this may be a key advantage of CMR-FT as re-analysis of the same images is known to underestimate the variability of STE GLS [36]. Furthermore, regarding conventional parameters, CMR has been shown to have substantially superior reproducibility over 2D echocardiography [37].

5. Conclusions

Comparison of strain analysis using CMR-FT and STE in a large population of acute ischaemic heart disease patients found similar feasibility between both techniques and good agreement of GLS, with slightly lower absolute values for CMR-FT. Agreement of segmental strain was only moderate, and segmental strain values from both techniques should therefore be compared with caution. Finally, CMR-FT revealed excellent reproducibility, both at a global and segmental level, which supports its robustness and use in clinical practice.

Funding

This work was supported by the Instituto de Salud Carlos III, Institute of Health, Ministry of Science, Spain, grant number EC07/90511 and RETICS RD06/0014/0025.

Declaration of Competing Interest

The authors declare that they have no known competing financial interests or personal relationships that could have appeared to influence the work reported in this paper.

Appendix A. Supplementary material

Supplementary data to this article can be found online at <https://doi.org/10.1016/j.ijcha.2020.100560>.

References

- [1] M. Saito, H. Okayama, T. Yoshii, et al., Clinical significance of global two-dimensional strain as a surrogate parameter of myocardial fibrosis and cardiac events in patients with hypertrophic cardiomyopathy, *Eur. Heart J. Cardiovasc. Imaging* 13 (7) (2012) 617–623.
- [2] J.-F. Hsiao, Y. Koshino, C.R. Bonnicksen, et al., Speckle tracking echocardiography in acute myocarditis, *Int. J. Cardiovasc. Imaging* 29 (2) (2013) 275–284.

- [3] D. Phelan, P. Collier, P. Thavendiranathan, et al., Relative apical sparing of longitudinal strain using two-dimensional speckle-tracking echocardiography is both sensitive and specific for the diagnosis of cardiac amyloidosis, *Heart* 98 (19) (2012) 1442–1448, LP.
- [4] A.C.T. Ng, E.A. Pihadi, M.L. Antoni, et al., Left ventricular global longitudinal strain is predictive of all-cause mortality independent of aortic stenosis severity and ejection fraction, *Eur. Hear. J. Cardiovasc. Imaging* 19 (8) (2018) 859–867.
- [5] J.C. Plana, M. Galderisi, A. Barac, et al., Expert consensus for multimodality imaging evaluation of adult patients during and after cancer therapy: a report from the ASE and the EACVI, *Eur. Heart J. Cardiovasc. Imaging* 15 (10) (2014) 1063–1093.
- [6] G.-P. Diller, A. Kempny, E. Liodakis, et al., Left ventricular longitudinal function predicts life-threatening ventricular arrhythmia and death in adults with repaired tetralogy of fallot, *Circulation* 125 (20) (2012) 2440–2446.
- [7] M.L. Antoni, S.A. Mollema, V. Delgado, et al., Prognostic importance of strain and strain rate after acute myocardial infarction, no. April, 2018, pp. 1640–1647.
- [8] Na Wang, Chung-Lieh Hung, Sung-Hee Shin, Brian Claggett, Hicham Skali, Jens Jakob Thune, Lars Køber, Amil Shah, John J.V. McMurray, Marc A. Pfeffer, Scott D. Solomon, Regional cardiac dysfunction and outcome in patients with left ventricular dysfunction, heart failure, or both after myocardial infarction, *Eur. Heart J.* 37 (5) (2016) 466–472, <https://doi.org/10.1093/eurheartj/ehv558>.
- [9] Kenneth Mangion, Christie McComb, Daniel A. Auger, Frederick H. Epstein, Colin Berry, Magnetic resonance imaging of myocardial strain after acute ST-segment-elevation myocardial infarction: a systematic review, *Circ. Cardiovasc. Imaging* 10 (8) (2017), <https://doi.org/10.1161/CIRCIMAGING.117.006498>.
- [10] D. García-dorado, B. García-del-blanco, I. Otaegui, et al., Intracoronary injection of adenosine before reperfusion in patients with ST-segment elevation myocardial infarction: a randomized controlled clinical trial ☆, *Int. J. Cardiol.* 177 (3) (2014) 935–941.
- [11] P.G. Steg, S.K. James, D. Atar, et al., ESC Guidelines for the management of acute myocardial infarction in patients presenting with ST-segment elevation, *Eur. Heart J.* 33 (20) (2012) 2569–2619.
- [12] A. Evangelista, F. Flachskampf, P. Lancellotti, et al., EAE recommendations for standardization of performance, digital storage and reporting of echocardiographic studies, *Eur. J. Echocardiogr.* 9 (4) (2008) 438–448.
- [13] R.M. Lang, M. Bierig, R.B. Devereux, et al., Recommendations for chamber quantification: a report from the ASE's guidelines and standards committee and the Chamber Quantification Writing Group, developed in conjunction with the EAE, *J. Am. Soc. Echocardiogr.* 18 (12) (2005) 1440–1463.
- [14] R.O. Mada, P. Lysyansky, A.M. Daraban, J. Duchenne, J.U. Voigt, How to define end-diastole and end-systole? Impact of timing on strain measurements, *JACC Cardiovasc. Imaging* 8 (2) (2015) 148–157.
- [15] J. Schulz-Menger, D.A. Bluemke, J. Bremerich, et al., Standardized image interpretation and post processing in cardiovascular magnetic resonance: SCMR Board of Trustees Task Force on Standardized Post Processing, *J. Cardiovasc. Magn. Reson.* 15 (1) (2013) 35.
- [16] J.M. Bland, D.G. Altman, Measuring agreement in method comparison studies, *Stat. Methods Med. Res.* 8 (2) (Apr. 1999) 135–160.
- [17] L. Portney, M. Watkins, *Foundations of clinical research: applications to practice*, third ed., New Jersey.
- [18] G. Pedrizzetti, P. Claus, P.J. Kilner, E. Nagel, Principles of cardiovascular magnetic resonance feature tracking and echocardiographic speckle tracking for informed clinical use, *J. Cardiovasc. Magn. Reson.* 18 (1) (2016) 51.
- [19] A. Bistoquet, J. Oshinski, O. Skrinjar, Left ventricular deformation recovery from cine MRI using an incompressible models, *IEEE Trans. Med. Imaging* 26 (9) (2007) 1136–1153.
- [20] O. Mirea, E.D. Pagourelis, J. Duchenne, et al., Variability and reproducibility of segmental longitudinal strain measurement: a report from the EACVI-ASE strain standardization task force, *JACC Cardiovasc. Imaging* 11 (1) (2018) 15–24.
- [21] M.M. Lamacie, P. Thavendiranathan, K. Hanneman, et al., Quantification of global myocardial function by cine MRI deformable registration-based analysis: comparison with MR feature tracking and speckle-tracking echocardiography, *Eur. Radiol.* 27 (4) (2017) 1404–1415.
- [22] T. Onishi, S.K. Saha, A. Delgado-Montero, et al., Global longitudinal strain and global circumferential strain by speckle-tracking echocardiography and feature-tracking cardiac magnetic resonance imaging: comparison with left ventricular ejection fraction, *J. Am. Soc. Echocardiogr.* 28 (5) (2018) 587–596.
- [23] Masaru Obokata, Yasufumi Nagata, Victor Chien-Chia Wu, Yuichiro Kado, Masahiko Kurabayashi, Yutaka Otsuji, Masaaki Takeuchi, Direct comparison of cardiac magnetic resonance feature tracking and 2D/3D echocardiography speckle tracking for evaluation of global left ventricular strain, *Eur. Heart J. Cardiovasc. Imaging* 17 (5) (2016) 525–532, <https://doi.org/10.1093/ehjci/jev227>.
- [24] A. Kempny, R. Fernández-Jiménez, S. Orwat, et al., Quantification of biventricular myocardial function using cardiac magnetic resonance feature tracking, endocardial border delineation and echocardiographic speckle tracking in patients with repaired tetralogy of fallot and healthy controls, *J. Cardiovasc. Magn. Reson.* 14 (1) (2012) 32.
- [25] D. Augustine, A.J. Lewandowski, M. Lazdam, et al., Global and regional left ventricular myocardial deformation measures by magnetic resonance feature tracking in healthy volunteers: comparison with tagging and relevance of gender, *J. Cardiovasc. Magn. Reson.* 15 (2013) 1.
- [26] LiNa Wu, Tjeerd Germans, Ahmet Güçlü, Martijn W Heymans, Cornelis P Allaart, Albert C van Rossum, Feature tracking compared with tissue tagging measurements of segmental strain by cardiovascular magnetic resonance, *J. Cardiovasc. Magn. Reson.* 16 (1) (2014), <https://doi.org/10.1186/1532-429X-16-10>.
- [27] M. Aurich, M. Keller, S. Greiner, et al., Left ventricular mechanics assessed by two-dimensional echocardiography and cardiac magnetic resonance imaging: comparison of high-resolution speckle tracking and feature tracking, *Eur. Heart J. Cardiovasc. Imaging* 17 (12) (2016) 1370–1378.
- [28] S. Orwat, A. Kempny, G.-P. Diller, et al., Cardiac magnetic resonance feature tracking—a novel method to assess myocardial strain: Comparison with echocardiographic speckle tracking in healthy volunteers and in patients with left ventricular hypertrophy, *Kardiol. Pol. (Polish Hear Journal)* 72 (4) (2014) 363–371.
- [29] J. Gavara, J.F. Rodriguez-Palomares, F. Valente, et al., Prognostic value of strain by tissue tracking cardiac magnetic resonance after ST-segment elevation myocardial infarction, *JACC Cardiovasc. Imaging* (2017).
- [30] Jie Wang, Weihao Li, Jiayu Sun, Hong Liu, Yu Kang, Dan Yang, Liuyu Yu, Andreas Greiser, Xiaoyue Zhou, Yuchi Han, Yucheng Chen, Improved segmental myocardial strain reproducibility using deformable registration algorithms compared with feature tracking cardiac MRI and speckle tracking echocardiography: Segmental Myocardial Strain Using DRA, *J. Magn. Reson. Imaging* 48 (2) (2018) 404–414, <https://doi.org/10.1002/jmri.25937>.
- [31] A. Thorstensen, H. Dalen, B.H. Amundsen, S.A. Aase, A. Stoylen, Reproducibility in echocardiographic assessment of the left ventricular global and regional function, the HUNT study, *Eur. J. Echocardiogr.* 11 (2) (2010) 149–156, <https://doi.org/10.1093/ejehocard/jep188>.
- [32] H. Baumgartner, V. Falk, J.J. Bax, et al., 2017 ESC/EACTS Guidelines for the management of valvular heart disease, vol. 38, no. 36. 2017.
- [33] J.L. Zamorano, P. Lancellotti, D.R. Muñoz, et al., 2016 ESC position paper on cancer treatments and cardiovascular toxicity developed under the auspices of the ESC committee for practice guidelines: the task force for cancer treatments and cardiovascular toxicity of the ESC, *Russ. J. Cardiol.* 143 (3) (2017) 105–139.
- [34] P. Ponikowski, A.A. Voors, S.D. Anker, et al., 2016 ESC Guidelines for the diagnosis and treatment of acute and chronic heart failure, *Eur. Heart J.* 37 (27) (2016) 2129–2200m.
- [35] G. Montalescot, U. Sechtem, S. Achenbach, et al., 2013 ESC guidelines on the management of stable coronary artery disease, *Eur. Heart J.* 34 (38) (2013) 2949–3003.
- [36] K.E. Farsalinos, A.M. Daraban, S. Ünlü, J.D. Thomas, L.P. Badano, J.U. Voigt, Head-to-Head Comparison of Global Longitudinal Strain Measurements among Nine Different Vendors: The EACVI/ASE Inter-Vendor Comparison Study, *J. Am. Soc. Echocardiogr.* 28 (10) (2015) 1171–1181.
- [37] F. Grothues, G.C. Smith, J.C.C. Moon, et al., Comparison of Interstudy Reproducibility of Cardiovascular Magnetic Resonance With Two-Dimensional Echocardiography in Normal Subjects and in Patients With Heart Failure or Left Ventricular Hypertrophy, vol. 9149, no. 02, pp. 29–34.